

Abundance of microbial genes associated with nitrogen cycling as indices of biogeochemical process rates across a vegetation gradient in Alaska

Dorthe Groth Petersen,^{1*} Steven J. Blazewicz,¹
Mary Firestone,¹ Donald J. Herman,¹
Merritt Turetsky² and Mark Waldrop³

¹The Department of Environmental Science, Policy, and Management, 137 Mulford Hall, University of California, Berkeley, CA 94720, USA.

²Integrative Biology, University of Guelph, 50 Stone Road East, Guelph, Ontario, Canada.

³United States Geological Survey, 345 Middlefield Road, MS 962, Menlo Park, CA 94025, USA.

Summary

Nitrification and denitrification processes are crucial to plant nutrient availability, eutrophication and greenhouse gas production both locally and globally. Unravelling the major environmental predictors for nitrification and denitrification is thus pivotal in order to understand and model environmental nitrogen (N) cycling. Here, we sampled five plant community types characteristic of interior Alaska, including black spruce, bog birch, tussock grass and two fens. We assessed abundance of functional genes affiliated with nitrification (bacterial and archaeal *amoA*) and denitrification (*nirK/S* and *nosZ*) using qPCR, soil characteristics, potential nitrification and denitrification rates (PNR and PDR) and gross mineralization rates. The main chemical and biological predictors for PNR and PDR were assigned through path analysis. The potential N cycling rates varied dramatically between sites, from some of the highest (in fens) to some of the lowest (in black spruce) measured globally. Based on path analysis, functional gene abundances were the most important variables to predict potential rates. PNR was best explained by bacterial *amoA* gene abundance followed by ammonium content, whereas PDR was best explained directly by *nosZ* gene abundance and indirectly by *nirK/S* gene

abundance and nitrate. Hence, functional gene abundance is a valuable index that integrates recent environmental history and recent process activity, and therefore is a good predictor of potential rates. The results of this study contribute to our understanding of the relative importance of different biological and chemical factors in driving the potential for nitrification and denitrification across terrestrial ecosystems.

Introduction

Nitrification and denitrification processes are important in soil nitrogen (N) cycling, as they lead to mobile forms of N for plant uptake, N leaching and gaseous losses from the soil system. Both processes are important sources of atmospheric N₂O (Mosier, 1998), which has become the largest ozone-depleting substance emitted through human activities (Ravishankara *et al.*, 2009). N₂O has a global warming potential approximately 296 times higher than a molar equivalent of carbon dioxide (CO₂) over a 100 year horizon (Prather *et al.*, 2001). Hence nitrification and denitrification are not only important to the local soil environment, but also to the global environment, and it is important that we are able to predict large differences in these process rates across ecosystems.

Nitrification is the two-step process in which ammonia (NH₃) is oxidized to nitrite (NO₂⁻) and nitrate (NO₃⁻). The *amoA* gene, which codes for the ammonia monooxygenase enzyme used in the first step of ammonia oxidation, has been used extensively as a molecular marker gene for cultivation-independent studies of ammonia oxidizing bacteria (AOB) and archaea (AOA) in soil systems (e.g. Carney *et al.*, 2004; Leininger *et al.*, 2006). Functional roles of AOB and AOA have been analysed by correlating abundances of the *amoA* genes to nitrification rates in soils and sediments (Jia and Conrad, 2009; Mertens *et al.*, 2009; Bernhard *et al.*, 2010).

Denitrification is the sequential reduction of soluble nitrate, through nitrite and nitric oxide (NO) to gaseous nitrous oxide (N₂O) and eventually dinitrogen (N₂). The ability to reduce nitrate is widespread among several phylogenetic groups (Zumft, 1997). This makes a functional gene approach to studying this process preferable, which allows for characterization and quantification of a group of

Received 6 May, 2011; revised 14 November, 2011; accepted 22 November, 2011. *For correspondence. E-mail dorthe.petersen@biology.au.dk; Tel. (+45) 8942 2663; Fax (+45) 8942 2722. [†]Present address: Center for Geomicrobiology, Department of Bioscience, Aarhus University, Ny Munkegade 114, DK-8000 Aarhus C, Denmark. The work was conducted at University of California, Berkeley, CA 94720, USA.

functionally similar organisms. Here, we focus on the second and the last step of denitrification, namely nitrite reduction and nitrous oxide reduction. Nitrite reduction is linked to the *nirK* and *nirS* genes encoding structurally different but functionally similar nitrite reductases. The *nosZ* gene codes for nitrous oxide reductase which is active during the final step of denitrification, i.e. the reduction of N_2O to N_2 (Zumft, 1997).

Boreal ecosystems represent a unique opportunity to study N cycling processes because of the dramatic differences in plant communities within small geographical areas. The most dominant vegetation cover in interior Alaska is black spruce (*Picea mariana*), and black spruce forests generally exhibit low rates of N mineralization due to low soil pH, low temperatures and poor litter quality (for example Giblin *et al.*, 1991; Van Cleve *et al.*, 1993). In contrast, fens, which also comprise a large component of northern wetlands, can have low rates of net nitrification (Bayley *et al.*, 2005), but rates of denitrification can be high due to high organic matter (OM) content and anoxic conditions (Wray and Bayley, 2007). Thus, rates of N cycling processes can differ dramatically among geographically close plant communities in the region. Microbially mediated N cycling in soil is affected by environmental factors most notably moisture content, temperature, oxygen availability, pH and supply of OM and inorganic N compounds (Wallenstein *et al.*, 2006 and references herein). Diversity and abundance of N cycling microorganisms have also been shown to affect N cycling rates, but causal relationships between these biological variables and N cycling rates are difficult to predict (Wallenstein *et al.*, 2006; Wankel *et al.*, 2011).

The main objective of this study was to evaluate which environmental factors were important in explaining measured patterns in potential N cycling rates in soils across five major plant community types in interior Alaska. More specifically, we tested whether potential rates of nitrification (PNR) and denitrification (PDR) were predictable solely based on chemical characteristics [e.g. pH, water content, dissolved organic carbon (DOC), nitrate and ammonium content], or whether biological variables (e.g. abundance of functional microbial groups based on quantitative PCR) added additional explanatory power to the analysis. Direct and indirect relationships between functional groups of microorganisms, soil chemistry and process rates were examined using path analysis. We developed three hypothetical, competing path models using chemical/physical and biological variables to explain changes in potential rates of nitrification and denitrification (Fig. 1). The models describe (a) a simple relationship where microbial gene abundances are exclusively the best direct predictors of potential rates and chemical/physical characteristics act indirectly on potential rates by affecting gene abundances (linear model); (b)

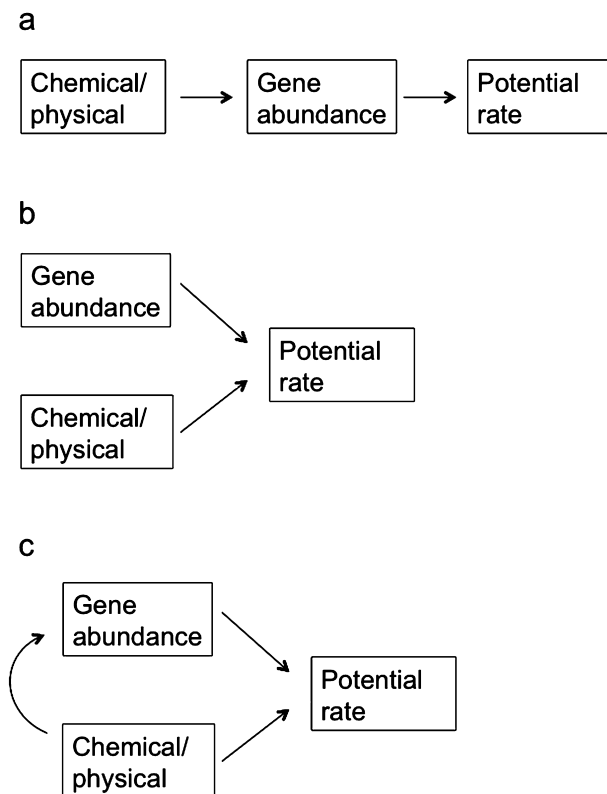


Fig. 1. Conceptual models to describe the influence of chemical/physical characteristics and microbial gene abundance on potential N cycling rates. Model (a) describes a simple linear model where the chemical characteristics affect potential rates indirectly through microbial gene abundance. Model (b) illustrates a direct model where both the chemical characteristics and microbial gene abundances directly affect potential rates, but without interactions between the chemistry and microbiology. Finally, model (c) describes a more complex mixed model where chemical characteristics as well as gene abundances directly affect potential rates, but there are also interactions between the chemical characteristics and the microbial gene abundances, which allows for indirect effects to occur.

both chemical/physical characteristics and microbial gene abundances directly affect potential rates but do not interact (direct model); and (c) chemical/physical characteristics and microbial gene abundances directly affect potential rates but do interact (mixed model). To determine which model, if any, best fits our experimental data, we developed full path models for PNR and PDR including all relevant experimental variables, and we conducted stepwise alterations of the models using a nested model approach until the best model fit was found where all paths between variables were statistically significant.

Results

Soil characteristics across the gradient

This study was conducted with soils sampled across five lowland plant communities characteristic to interior

Alaska, and the sites included a black spruce forest overlying permafrost, a bog birch site also over permafrost dominated by shrubs, a tussock grass site with large and deep (~0.5 m) interspaces, an emergent fen site and finally a rich fen site (see *Experimental procedures*). Soil moisture increased along the transect from the black spruce forest out into the saturated rich fen. For the other sites (emergent fen, tussock area and bog birch), water table was 10 cm below the surface at the time of sampling and, at the black spruce site, the water table was below 15 cm. Bulk densities varied significantly between the sites, thus all variables are expressed per area (m^{-2}) to make comparisons relevant at the ecosystem scale. Dissolved organic carbon averaged 5.9 g m^{-2} in the emergent fen to 8.7 g m^{-2} at the tussock site which was higher than the black spruce, rich fen and the bog birch sites. Dissolved organic nitrogen (DON) contents ranged from 4.7 to 9.2 g m^{-2} across the sites and did not differ among sites (see Table 1 for all variables). Nitrate and ammonium contents (KCl extractions) were highly correlated (Table 2), with the highest values at the emergent fen site (2.6 and 2.9 g m^{-2} respectively), and the lowest at the black spruce site (0.4 and 0.2 g m^{-2} respectively). No significant differences were found between sites for soil OM contents or pH in the surface 15 cm (Table 1).

Rates of nitrogen cycling

Overall, the rates of N cycling were lowest at the forested sites, and highest at the fens and tussock sites. Gross N mineralization rates (isotope pool dilution technique) ranged from $39.5 \text{ mg N m}^{-2} \text{ h}^{-1}$ at the black spruce site to $339.5 \text{ mg N m}^{-2} \text{ h}^{-1}$ at the rich fen site (Fig. 2) and they were significantly correlated with soil water contents, PNR and PDR across sites (Table 2). PNR and PDR were highly correlated ($r = 0.866$, $P = 0.0001$) with lowest rates at the black spruce site (1.26 and $1.29 \text{ mg N m}^{-2} \text{ h}^{-1}$ respectively) and highest rates at the emergent fen (18.03 and $287.06 \text{ mg N m}^{-2} \text{ h}^{-1}$) (Figs. 3 and 4).

Abundance of soil bacteria and archaea

To compare potential and gross rates of nitrogen cycling with the presence of microorganisms in the five soils across the gradient, we quantified the abundances of several genes using quantitative PCR (qPCR). The 16S rRNA gene was used to assess the abundance of total bacteria and archaea, whereas several functional genes were used to assess abundance of different functional groups of N cycling microorganisms. The *amoA* gene was used to quantify bacterial and archaeal ammonia oxidizers and *nirK*, *nirS* and *nosZ* genes were used to quantify different groups of denitrifiers. Throughout this paper, the abundance of genes will be used instead of abundance of

Table 1. Soil characteristics of replicate samples along the gradient ($n = 5$, average with standard error in parenthesis).

Site	Bulk density ($\text{mg dry soil cm}^{-3}$)	Water content (g water per g dry soil)	Organic matter (mg/kg)	pH	DOC (g m^{-2})	DON (g m^{-2})	NO_3^- (g m^{-2})	NH_4^+ (g m^{-2})
Black spruce	17.2 (4.8) ^C	2.8 (1.3) ^B	855.3 (38.0) ^A	4.8 (0.5) ^A	7.5 (2.4) ^{AB}	5.9 (2.8) ^A	0.4 (0.1) ^B	0.2 (0.04) ^B
Bog birch	26.3 (12.4) ^{ABC}	4.5 (1.0) ^B	767.2 (104.4) ^{AB}	4.3 (0.2) ^A	6.9 (0.8) ^{AB}	4.7 (3.6) ^A	0.4 (0.1) ^B	0.2 (0.01) ^B
Tussock	35.4 (14.0) ^A	4.3 (1.3) ^B	597.5 (77.3) ^C	4.7 (0.3) ^A	8.7 (1.0) ^A	9.2 (9.2) ^A	0.7 (0.07) ^B	1.5 (0.2) ^{AB}
Emergent fen	35.7 (3.1) ^{AB}	3.7 (3.3) ^B	637.1 (80.1) ^{BC}	4.5 (0.4) ^A	5.9 (1.3) ^B	5.9 (7.3) ^A	2.6 (0.5) ^A	2.9 (0.9) ^A
Rich fen	23.1 (4.3) ^{BC}	7.8 (1.2) ^A	766.7 (36.5) ^{AB}	4.7 (0.4) ^A	6.3 (1.4) ^{AB}	4.9 (6.3) ^A	0.6 (0.07) ^B	1.1 (0.2) ^B

Capital letters denote significant differences between sites ($P < 0.05$, ANOVA with Tukey's HSD) for each variable.

Table 2. Correlation table with all measured variables.

	PDR	Water content	OM	Ammonium	Nitrate	Archaea	AOB	AOA	<i>nosZ</i>	Bacteria	Gross min	DOC	PNR	DON
Water content	-0.004 (0.987)													
OM	0.669 (0.0003)	-0.244 (0.238)												
Ammonium	0.592 (0.001)	0.021 (0.918)	0.528 (0.006)											
Nitrate	0.569 (0.003)	-0.166 (0.425)	0.456 (0.021)	0.857 (< 0.0001)										
Archaea	0.172 (0.412)	0.557 (0.003)	0.072 (0.721)	0.166 (0.425)	0.025 (0.902)									
AOB	0.852 (< 0.0001)	-0.101 (0.636)	0.542 (0.006)	0.688 (0.0004)	0.668 (0.0002)	0.109 (0.611)								
AOA	0.377 (0.069)	-0.160 (0.453)	0.606 (0.002)	0.287 (0.173)	0.269 (0.203)	-0.020 (0.922)	0.337 (0.115)							
<i>nosZ</i>	0.9 (< 0.0001)	-0.079 (0.706)	0.701 (< 0.0001)	0.654 (0.0004)	0.716 (< 0.0001)	0.160 (0.444)	0.839 (< 0.0001)	0.416 (0.043)						
Bacteria	0.818 (< 0.0001)	0.041 (0.843)	0.813 (< 0.0001)	0.541 (0.005)	0.491 (0.012)	0.360 (0.076)	0.622 (0.001)	0.605 (0.001)	0.843 (< 0.0001)					
Gross min	0.617 (0.001)	0.509 (0.011)	0.471 (0.020)	0.641 (0.0007)	0.506 (0.011)	0.621 (0.001)	0.597 (0.002)	0.329 (0.125)	0.637 (0.0008)	0.703 (0.0001)				
DOC	0.042 (0.338)	0.029 (0.425)	0.009 (0.659)	0.000 (0.881)	0.048 (0.302)	0.025 (0.561)	0.000 (0.993)	0.080 (0.189)	0.071 (0.206)	0.000 (0.940)	0.038 (0.371)			
PNR	0.866 (< 0.0001)	0.001 (0.995)	0.529 (0.007)	0.770 (< 0.0001)	0.756 (< 0.0001)	0.099 (0.636)	0.842 (< 0.0001)	0.273 (0.196)	0.863 (< 0.0001)	0.607 (0.001)	0.669 (0.0003)	0.065 (0.229)		
DON	0.234 (0.261)	-0.191 (0.362)	0.275 (0.182)	0.314 (0.125)	0.103 (0.624)	-0.038 (0.853)	0.252 (0.233)	0.318 (0.129)	0.229 (0.269)	0.338 (0.097)	0.180 (0.398)	0.328 (0.003)	0.199 (0.338)	
<i>nirK/S</i>	0.733 (< 0.0001)	0.006 (0.978)	0.473 (0.017)	0.286 (0.164)	0.443 (0.026)	0.204 (0.327)	0.54 (0.006)	0.179 (0.401)	0.837 (< 0.0001)	0.633 (0.0007)	0.522 (0.008)	0.163 (0.051)	0.719 (< 0.0001)	-0.035 (0.867)

The strength of the linear relationship between two variables is described by the Pearson Product Moment Correlation Coefficient, *r*, and negative numbers correspond to negative correlations. *P*-values are given in parenthesis and significant values are written in italics. Variables in the table are water content (g g⁻¹), ammonium and nitrate (g m⁻²), OM = organic matter (μg g⁻¹), PNR = potential nitrification rate (mg N m⁻² h⁻¹), PDR = potential denitrification rate (mg N m⁻² h⁻¹), gross min = gross mineralization (mg N m⁻² h⁻¹), archaea = number of archaeal 16S rRNA genes, AOB = number of bacterial *amoA* genes, AOA = number of archaeal *amoA* genes, *nosZ* = number of *N*₂O reductase genes, *nirK/S* = number of nitrate reductase gene, DON = dissolved organic nitrogen (g m⁻²). pH did not correlate significantly with any variables and have not been included in this table (*P* > 0.05).

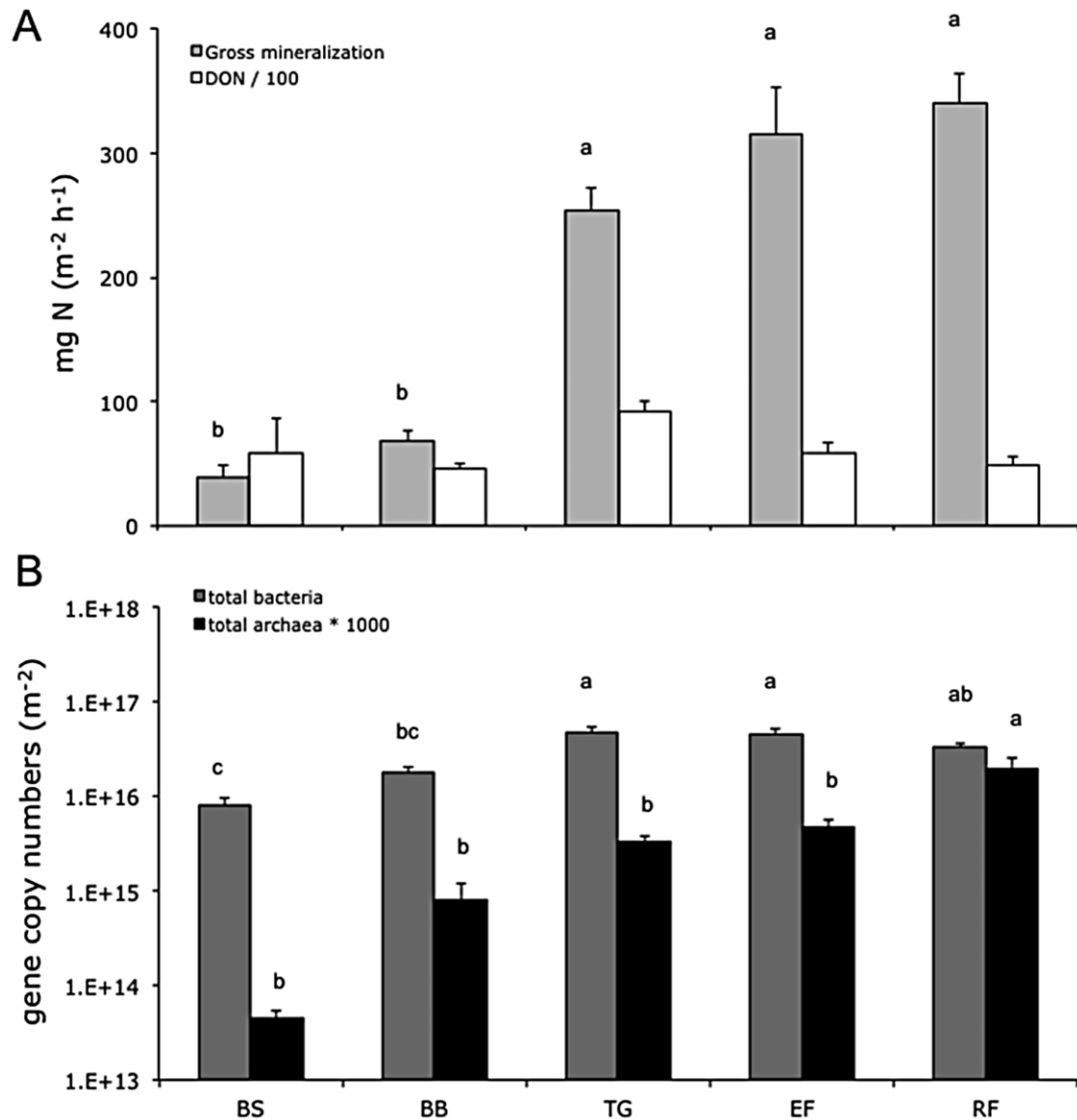


Fig. 2. (A) Rates of gross mineralization (grey bars) and DON concentration divided by 100 (mg N m⁻²) (white bars), and (B) abundances of total bacterial 16S rRNA genes (dark grey bars) and archaeal 16S rRNA genes multiplied by 1000 (black bars) across the five sites (BS: black spruce, BB: bog birch, TG: tussock grass, EF: emergent fen and RF: rich fen). Bars represent average values ± 1 SE ($n = 5$), and letters above each column describes differences between sites (ANOVA with Tukey's *post hoc* test, $P < 0.05$). No significant differences were found between sites for DON.

organisms, since such a calculation is based on a theoretical average number of functional gene copies per microorganism.

The abundance of bacterial 16S rRNA genes was significantly higher (3–5 orders of magnitude) than the abundance of archaeal 16S rRNA genes across all sites (Student's *t*-test, $P < 0.05$, $n = 25$). The abundance of bacterial 16S rRNA genes was in the range of 8.1×10^{11} (BS) to 2.0×10^{12} (EF) genes/g soil, whereas the abundance of archaeal 16S rRNA genes ranged from 5.9×10^6 (BS) to 6.6×10^8 (RF) genes/g soil. Bacterial 16S rRNA

gene abundance was significantly lower at the black spruce and bog birch sites compared with the remaining sites. This was not the case for archaeal 16S rRNA gene abundance, which was highest at the rich fen (ANOVA with Tukey's HSD test, $P < 0.05$, $n = 5$) (Fig. 2B). Both bacterial and archaeal 16S rRNA gene abundances correlated with gross N mineralization rates (Table 2).

Across all sites, the abundance of bacterial *amoA* genes was 8–18 times higher than the abundance of archaeal *amoA* genes. This trend was significant at the rich fen, emergent fen, and bog birch sites (students

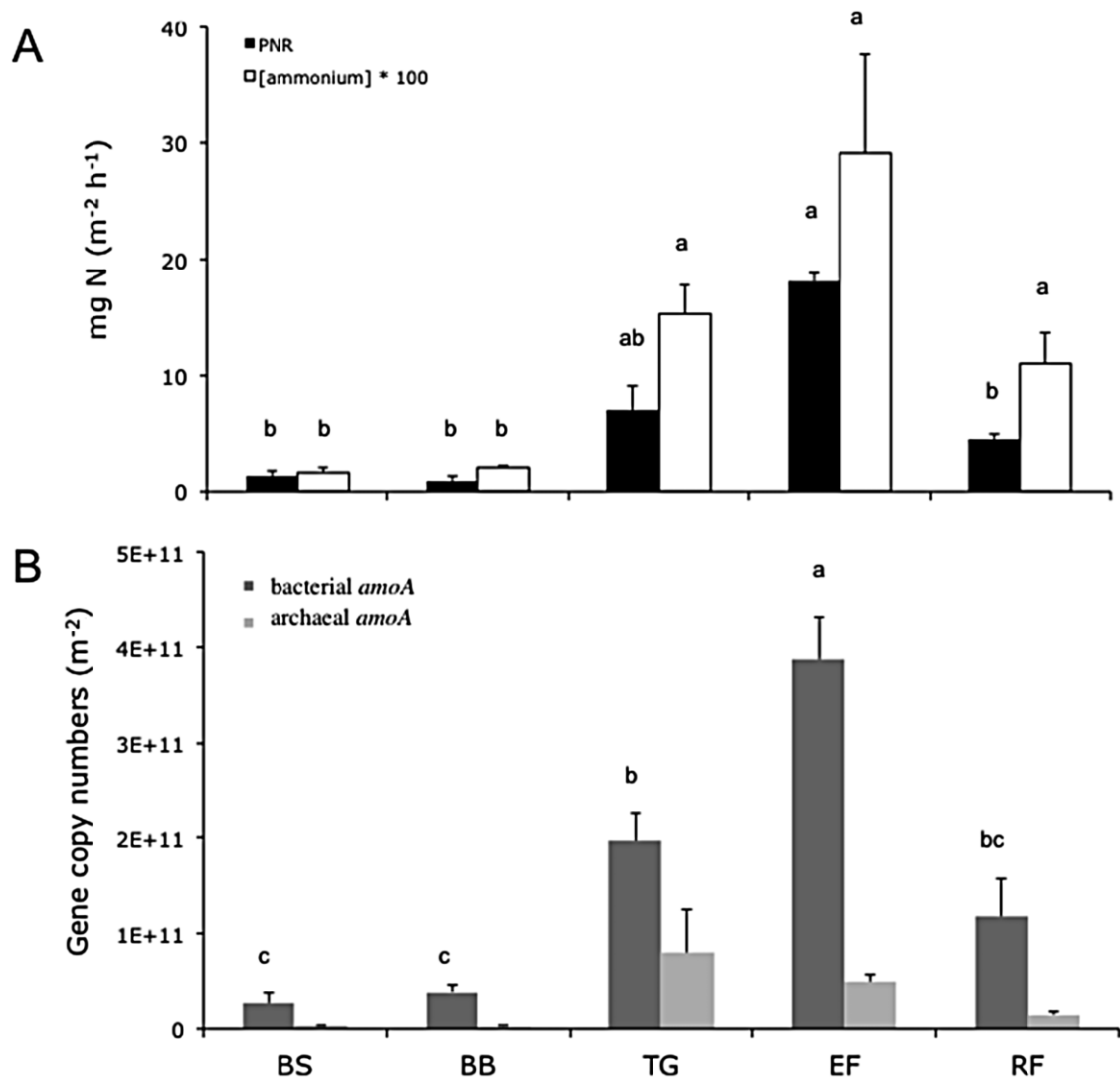


Fig. 3. (A) Potential nitrification rates (PNR) (mg N m⁻² h⁻¹) (black bars) and soil ammonium content divided by 100 (mg N/m²) (white bars). (B) Gene copy numbers of bacterial *amoA* genes (AOB) (dark grey bars) and archaeal *amoA* genes (AOA) (light grey bars) across all five sites (BS: black spruce, BB: bog birch, TG: tussock grass, EF: emergent fen and RF: rich fen). Bars represent averages + 1 SE ($n = 5$). Letters above bars represent differences between sites for each variable (ANOVA with Tukey's *post hoc* test) ($P < 0.05$). No significant differences were found between sites for archaeal *amoA* gene copy numbers.

t-test, $P < 0.05$, $n = 5$). The abundance of *amoA* genes from bacteria (AOB) was highest at the emergent fen, tussock, and rich fen and lower at the black spruce and bog birch sites (ANOVA with Tukey's HSD test, $P < 0.05$, $n = 5$) (Fig. 3B). In contrast, no significant differences appeared between sites for the *amoA* genes from ammonia oxidizing archaea (AOA) ($P > 0.05$, $n = 5$). We found a significant correlation between the abundance of bacterial *amoA* genes and PNR and ammonium content, whereas PNR and ammonium content did not correlate with abundance of archaeal *amoA* genes (Table 2).

As with the bacterial *amoA* gene distribution, we found distinct spatial patterns in the distribution of

genes involved in denitrification. The abundance of *nirS* genes was always significantly higher than the abundance of *nirK* genes for all stations, except for the bog birch site. For further analyses the abundance of *nirK* and *nirS* genes will be added due to their functionally similar properties and referred to as *nirK/S*. The abundance of *nosZ* genes was significantly higher than the *nirK/S* gene abundances across all five sites (Fig. 4B) (students *t*-test, $P < 0.05$, $n = 5$). We found significant correlations between abundance of *nosZ* and *nirK/S* genes and PDR, PNR, abundance of bacterial *amoA* genes and nitrate content (Table 2).

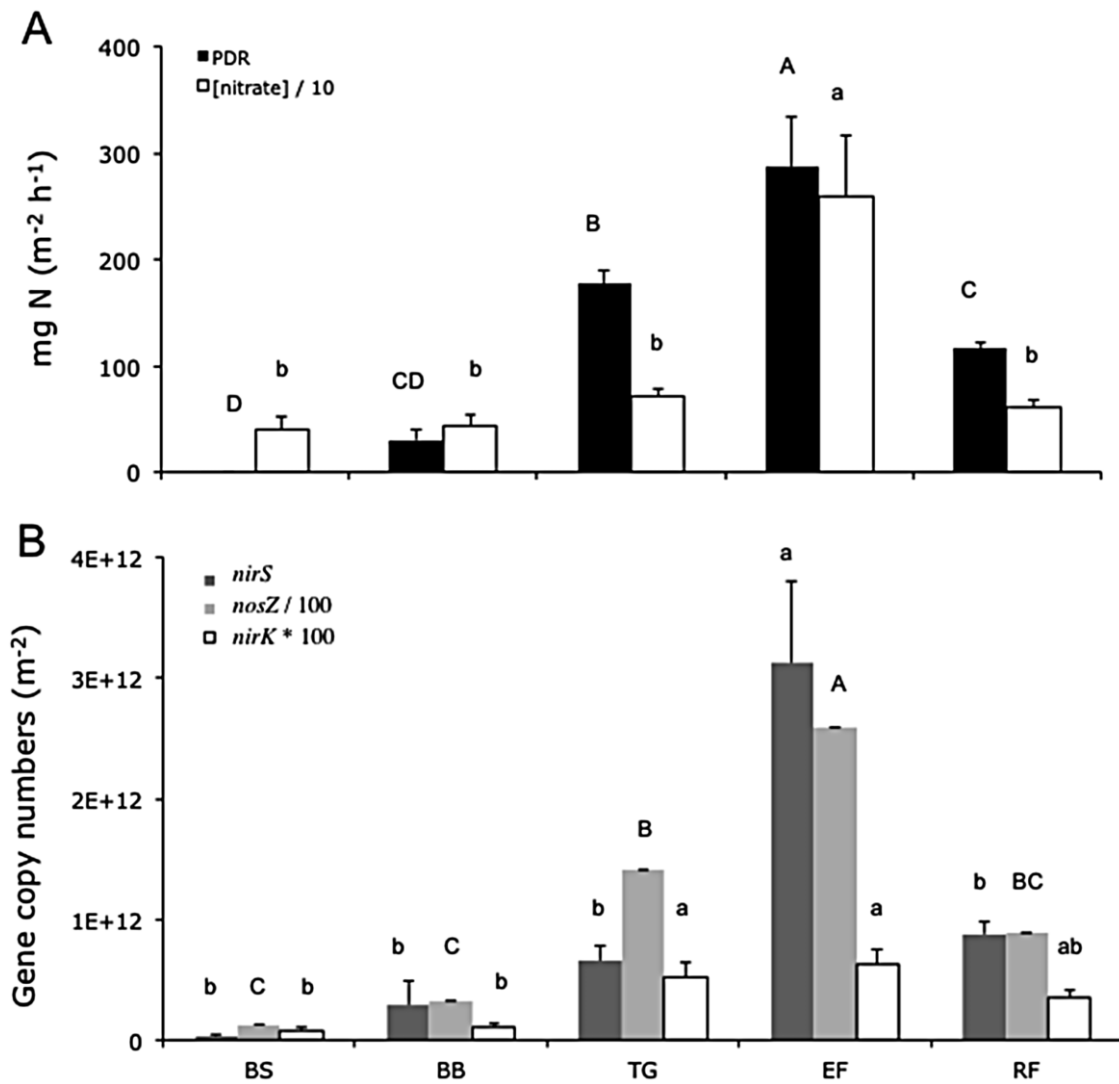


Fig. 4. (A) Potential denitrification rates (PDR) ($\text{mg N m}^{-2} \text{h}^{-1}$) (black bars) and soil nitrate content divided by 10 (mg N m^{-2}) (white bars), and (B) Gene copy numbers of *nirS* (dark grey bars), *nosZ* (divided by 100) (light grey bars), *nirK* (multiplied by 100) (white bars) across all sites in the gradient (BS: black spruce, BB: bog birch, TG: tussock grass, EF: emergent fen and RF: rich fen). Bars and lines represent averages + 1 SE ($n = 5$). Letters above bars represent differences between sites for each variable (ANOVA with Tukey's *post hoc* test) ($P < 0.05$).

Controlling factors for nitrogen cycling processes and microorganisms in the soils

In order to further explore relationships between measured physical/chemical and biological variables and PNR and PDR, we utilized stepwise multiple regressions (SMR) and path analysis, with all relevant variables included (see *Statistics* section for details and Fig. 5A). According to SMR, the significant variables that explained the largest part of the variation in PNR was abundance of bacterial *amoA* genes ($R^2 = 0.69$, $P < 0.00001$), and soil ammonium content (sum $R^2 = 0.79$, $P < 0.02$) explaining a total of 79% of the variation in the PNR data. The largest part of the variation in PDR was explained by *nosZ* gene

abundance ($R^2 = 0.79$, $P < 0.00001$) explaining a total of 79% of the variation in the PDR data (SMR, $n = 25$).

Path analyses indicated that the conceptual full models for PNR and PDR (Fig. 5A) fit the observed data well according to the model chi-squared (χ^2) statistic (PNR full model $\chi^2 = 5.159$, d.f. = 10, $P = 0.880$; PDR full model $\chi^2 = 19.413$, d.f. = 14, $P = 0.150$). NNFI (non-normed fit index, also known as Tucker–Lewis index) values supported that the full PNR and PDR models were well fitted to the data (PNR NNFI = 1.2, PDR NNFI = 0.91). After removing the non-significant paths (Fig. 5B), the reduced models were evaluated for goodness of fit. The much-simplified final models also fit the observed data well (PNR: $\chi^2 = 1.353$, d.f. = 4, $P = 0.852$, NNFI = 1.12; PDR:

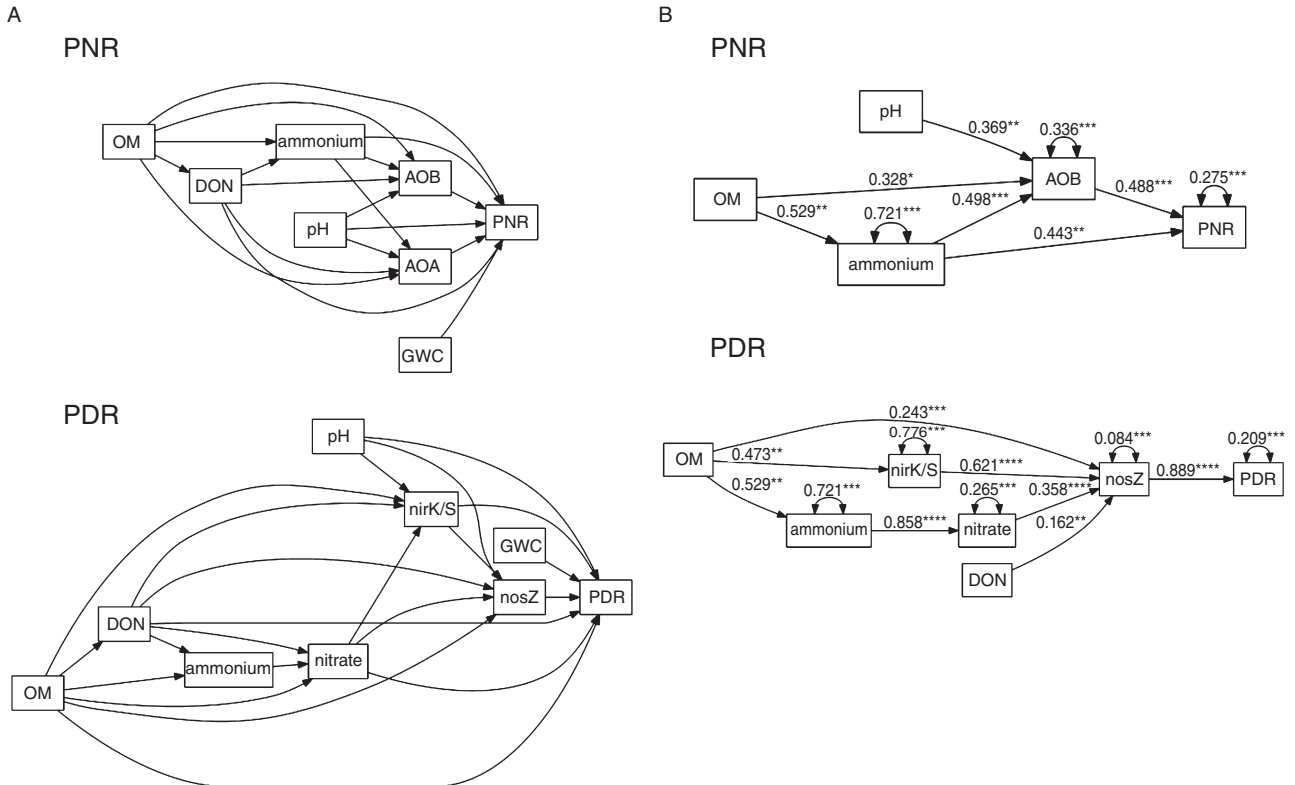


Fig. 5. Path diagrams representing the full model (A) and the final models (B) to describe the patterns observed in potential nitrification (PNR) and denitrification rates (PDR). Numbers associated with single headed arrows are partial regression coefficients of multiple regressions. Numbers associated with double-headed arrows represent unexplained variation ($1 - R^2$), which represents the effect of unmeasured variables and measurement error.

A. The full models included all relevant variables like electron donors, electron acceptors and abundance of relevant functional genes (see *Statistics* section for details).

B. Results from path analyses showing the effects of chemical and biological variables on PNR and PDR. All pathways in the final model are significant (* $P \leq 0.05$; ** $P \leq 0.01$; *** $P \leq 0.001$; **** $P \leq 0.0001$).

$\chi^2 = 17.280$, d.f. = 13, $P = 0.187$, NNFI = 0.952). Modification indexes were calculated for both final models to determine if adding or subtracting any parameters would improve the model fit, but changes to the models based on the largest modification indexes resulted in worse fits for both models (data not shown).

Since all of the paths and variables in the final models are present in the full models, the final models are considered nested models. Likelihood ratio test (LRT) is useful for comparing nested models to determine if the models are significantly different in their fit of the data. A comparison of full and final nested models for both PNR and PDR produced non-significant LRT χ^2 values (PNR LRT $\chi^2 > 3.806$, d.f. = 6, $\alpha = 0.05$; PDR LRT $\chi^2 > 2.133$, d.f. = 1, $\alpha = 0.05$), indicating that the models have statistically similar fits.

The comparative fit index (CFI) values were used to evaluate our full and final models and the values show that both models have similar fits (PNR CFI_{full} = 1, CFI_{final} = 1; PDR CFI_{full} = 0.963, CFI_{final} = 0.970) (0 = no fit, 1 = perfect fit). However, we consider the final models to

be superior since they equally explain variation in the dependent variables, are much simpler, and include only statistically significant paths. In accordance with SMR, the final model for PNR based on path analyses showed that bacterial *amoA* gene abundance (AOB) is the most important controlling factor for PNR followed by ammonium content. Furthermore, pH acts directly on AOB and OM acts on both AOB and the concentration of ammonium. For PDR, *nosZ* gene abundance is the single most important explanatory variable, and *nirK/S* gene abundance is the most important predictor of *nosZ* gene abundance followed by nitrate, OM and DON contents. Organic matter influences nitrate content through ammonium content (Fig. 5B).

Discussion

The predictive power of functional gene abundances (path analyses)

Across the soils from the five different plant communities used in this study, we found the abundances of bacterial

amoA genes and *nosZ* genes to be the variables that best explained the variation in PNR and PDR respectively (Fig. 5B). Our data highlight that the microbial populations are important in mediating biogeochemical processes, and are themselves being influenced by chemical factors such as contents of ammonium, nitrate and OM. Chemical factors were less correlated to potential process rates, but generally have large indirect influences through abundance of functional genes. Hence, chemical characteristics are less important in predicting the potential rates, possibly due to the transient nature of inorganic and organic compounds in these soil systems. Functional genes within microbial populations, on the other hand, may be less dynamic and at the same time reflect and integrate longer-term fluctuations in the chemical and physical environment. Thus, the abundance of functional genes is the best predictive variable and a major controlling factor for the potential biogeochemical rates measured in this study.

Our final PNR model from path analysis agrees with a modified version of the proposed conceptual mixed model (Fig. 1C), where functional gene abundances are the most important descriptive factor for potential rates, and chemical characteristics interact with gene abundances and to a smaller extent describe the pattern in potential rates. Interestingly, the PDR model agrees with the simpler linear model (Fig. 1A), where gene abundances (in our case *nosZ* and *nirK/S* genes) are the main descriptive variables indirectly being affected by environmental factors like nitrate, DON and OM content.

NosZ gene abundance was significantly correlated to PDR, which was also the case when studying N cycling in a long-term fertilization experiment (50 years) (Hallin *et al.*, 2009) and spatial patterns of denitrifier communities in a large-scale experiment (relative *nosZ* abundance) (Philippot *et al.*, 2009). Based on the path analysis, *nirK/S* gene abundances were also strong predictors for PDR through *nosZ* gene abundance, suggesting a tight link between nitrite reduction and N₂O reduction across the Alaskan ecosystem types. *NirS* and *nirK* gene abundances have previously been found to correlate to PDR (Chronakova *et al.*, 2009; Dong *et al.*, 2009; Cuhel *et al.*, 2010), and hence may also be important in predicting PDR.

On the contrary, several studies report that the abundances of genes involved in denitrification are not correlated to PDR measurements (Dandie *et al.*, 2008; Miller *et al.*, 2008; Baudoin *et al.*, 2009; Djigal *et al.*, 2010; Song *et al.*, 2010; Attard *et al.*, 2011). One common feature for all the latter studies where gene abundances did not correlate to PDR is that the range of PDR measured were small ranging from 1.2-fold (Djigal *et al.*, 2010) to fourfold variations (Song *et al.*, 2010), or the experimental incubation period was short (144 h) (Miller *et al.*, 2008). This

suggests that abundances of functional genes are not suitable for predicting small changes in PDR. In the studies where abundance of functional genes correlates to PDR, the changes in PDR are larger spanning from fivefold (Philippot *et al.*, 2009; Cuhel *et al.*, 2010) to 200- to 400-fold variation (Chronakova *et al.*, 2009; Dong *et al.*, 2009), which was comparable to our PDR range.

Based on our data and preceding literature, we propose that gene abundances of relevant functional genes can serve as ecological integrative tools to predict the capacity of an ecosystem to carry out a given process. Gene copy numbers will not likely provide information on real-time process rates since such rates are dependent on current environmental conditions. Stochastic fluctuations in environmental conditions can cause rapid changes in real-time process rates, but will not necessarily affect gene abundance. Gene copy numbers can however predict potential process rates as shown by our data and other investigations. Gene copy number as a predictor of potential process rates is likely to be most robust under 'steady state' conditions and when differences in process rates are large. A molecular index of potential rates across ecosystem types would be a valuable tool for large-scale ecosystem studies and for predicting effects on process rates of broad environmental changes for example global warming.

Gross mineralization across the gradient

The gross N mineralization rates at the five sites in the gradient ranged from $0.9 \pm 0.5 \text{ g N m}^{-2} \text{ day}^{-1}$ ($24.5 \pm 5.4 \text{ mg N kg}^{-1} \text{ day}^{-1}$) at the black spruce site to $8.1 \pm 1.3 \text{ g N m}^{-2} \text{ day}^{-1}$ ($64.6 \pm 4.5 \text{ mg N kg}^{-1} \text{ day}^{-1}$) at the rich fen. In general, the gross rates of N mineralization in the black spruce and bog birch sites were comparable to gross rates found in a lichen-rich dwarf shrub tundra in Siberia ($0.2 \text{ g N m}^{-2} \text{ day}^{-1}$) (Biasi *et al.*, 2008), a frost-boil tundra ecosystem in Siberia ($0.4 \text{ g N m}^{-2} \text{ day}^{-1}$) (Kaiser *et al.*, 2005) and deciduous forests in southwestern Sweden (average of 3 soils: $9 \text{ mg N kg}^{-1} \text{ day}^{-1}$) (Bengtsson *et al.*, 2003). The higher rates found at the tussock and fen sites were comparable to gross rates found in a riparian fen in Scandinavia ($28 \text{ mg N kg}^{-1} \text{ day}^{-1}$) (Ambus *et al.*, 1992), but lower than gross rates found in topsoils from balsam poplar and alder stands in the Tanana River floodplain, Bonanza Creek LTER, Alaska ($240 \text{ mg N kg}^{-1} \text{ day}^{-1}$) (Fierer *et al.*, 2001). The rate differences in gross nitrogen mineralization indicate that the rates of N-cycling are significantly greater in the tussock and fen sites. Interestingly, we found a tight link between the abundance of total bacterial 16S rRNA genes and gross N mineralization rates. Such a link may be expected, since bacteria are major biological catalysts of this process and since the supply of OM may not be

limiting in these soil systems. Hence gene abundances can also be predictors of gross rates, and not only potential rates in environmental samples

Dynamics of nitrification and ammonia oxidizing microorganisms

Across the gradient, nitrification hotspots were associated with the two fens and the tussock sites, and PNR of these hotspots equalled or exceeded rates from studies from other northern regions. The mean PNR from our sites were generally comparable to field net nitrification rates measured at a sedge meadow and a willow-herb hummock site in Alaska, where net rates ranged from 6 to 36 mg N m⁻² day⁻¹ respectively (Chapin, 1996). Potential nitrification rate was lowest at the black spruce site ($3.2 \pm 3.1 \mu\text{g N g}^{-1} \text{ day}^{-1}$ or $61.3 \pm 31.4 \text{ mg N m}^{-2} \text{ day}^{-1}$) and highest at the emergent fen ($19.6 \pm 2.1 \mu\text{g N g}^{-1} \text{ day}^{-1}$ or $432.6 \pm 43.6 \text{ mg N m}^{-2} \text{ day}^{-1}$), and those rates are comparable to PNR measured in a 27-year-old poplar alder stand near the Bonanza Creek Experimental Forest (approximately $17 \mu\text{g N g}^{-1} \text{ day}^{-1}$) (Klingensmith and Van Cleve, 1993). We were unable to find any studies on Alaskan soils combining gene abundances from bacterial and archaeal nitrifiers with PNR, but PNR and *amoA* gene abundances from our study were comparable to other studies using soils from alpine grasslands and meadows (Makarov *et al.*, 2003), fertilized agricultural soils (He *et al.*, 2007; Shen *et al.*, 2008) and forest and grassland soils (Hoffmann *et al.*, 2007). It should be acknowledged, that PNR was measured at pH of 7.2, and hence the obtained potential rates may not reflect what happens in the soils at *in situ* pH of about 4.5. However, we followed the standard practice of conducting nitrification potential assays at a pH of 7.2 in order to make comparisons with other studies more appropriate.

Ammonia oxidizing bacteria appear to be the main driver for potential nitrification since the abundance of bacterial *amoA* genes significantly correlated with PNR across the gradient. Interestingly, the abundance of bacterial *amoA* genes exceeded the abundance of archaeal *amoA* genes. In recent studies, the abundance of archaeal *amoA* genes often exceeds that of bacterial *amoA* genes in soil systems (Leininger *et al.*, 2006; Shen *et al.*, 2008; Jia and Conrad, 2009). However, bacterial *amoA* genes have been found to outnumber or equal archaeal *amoA* genes in soil ecosystems comparable to the sites from the present study. For example, in conifer stands in Oregon, USA (Boyle-Yarwood *et al.*, 2008) and California, USA (D.G. Petersen, unpubl. data) the abundances of bacterial *amoA* genes were higher than archaeal *amoA* genes. Also, bacterial *amoA* genes have been found to outnumber archaeal *amoA* genes in grass-

lands from New Zealand (Di *et al.*, 2009) and France (Le Roux *et al.*, 2008) as well as in an alfalfa agricultural field in Croatia (Babic *et al.*, 2008). An increasing number of studies show higher abundance of AOB than AOA in sediments, which may be highly comparable to our waterlogged soils (Wankel *et al.*, 2011 and references therein). Given that we found high AOB/AOA ratios across all boreal plant communities (whether forests, fens or grasslands), our data suggest that AOB may be better adapted to the Alaskan soil environment than AOA.

Dynamics of denitrification and denitrifying microorganisms

The potential denitrification rates in this study are among the highest that we have been able to find relative to published studies on temperate and high latitude wetlands and poorly drained environments. PDR in the Alaskan soils are comparable to potential rates found in an urban riparian zone in Baltimore, USA (Groffman and Crawford, 2003), but PDR from the present study often exceed potential rates from other studies with waterlogged soils by one or two orders of magnitude, including a poorly drained peat soil from Scotland (Wheatley and Williams, 1989), riparian soils from Georgia, USA (Ambus and Lowrance, 1991), and riparian fens in New Zealand (Schipper *et al.*, 1993). PDR in the above mentioned studies, as well as for our study, were all measured through a denitrification enzyme assay (DEA) with the addition of excess nitrate and a carbon source, except for one study where only nitrate was added (Schipper *et al.*, 1993). In order to better understand such hot-spots for denitrification we need to measure *in situ* rates of both nitrification and denitrification, but such measurements are challenging especially regarding denitrification rate measurements (Groffman *et al.*, 2006).

Several studies have suggested that *nirS* and *nirK* bearing microorganisms take up different niches in the environment or have different habitat preferences (Desnues *et al.*, 2007; Junier *et al.*, 2008; Smith and Ogram, 2008; Hallin *et al.*, 2009; Knapp *et al.*, 2009). Based on gene abundances, our data suggest that *nirS* bearing denitrifiers are better adapted to the waterlogged soils present at our sites than *nirK* bearing denitrifiers. This was previously hypothesized in a study where *nirS* bearing denitrifiers from wetlands were found to be sensitive to short-term drought simulations indicating an adaptation of *nirS* bearing denitrifiers to static wet soil environments (Kim *et al.*, 2008). In agreement with this, studies in comparably drier soils have found lower *nirS* abundances compared with *nirK* abundances (Babic *et al.*, 2008; Dandie *et al.*, 2008; Bremer *et al.*, 2009 and references herein), positive correlations between *nirS*

gene abundance and soil moisture (Philippot *et al.*, 2009) and high abundance of *nirS* genes in sediments (Nogales *et al.*, 2002; Abell *et al.*, 2010). Our work is thus consistent with *nirS* playing an important ecological role in environments with high water content.

Conclusions

The present study provides a thorough analysis of the best explanatory variables for patterns in potential nitrogen cycling processes across five different terrestrial ecosystem types in interior Alaska. Overall, our study shows that quantitative DNA-based functional group information can provide very important information regarding the pattern and rate of N cycling processes in the environment. We propose that gene abundances in the environment reflect quantitative relationships with process rates and provide information about biogeochemical cycling that is relevant on temporal scales similar to those of interest to field ecologists (weeks or months) as well as modellers. As such, quantitative DNA based tools could be used to track large-scale and long-term changes in patterns of biogeochemical cycling that may be difficult to assess using short term measurements of process rates (i.e. pool dilution, trace gas flux). The ability to freeze and store DNA based information is an additional benefit. In the context of global change, these tools could be an effective means by which to examine how changing plant communities, microbial communities and soil nutrient status interact to affect biogeochemical cycling rates.

Experimental procedures

Description of sites and sample collections

This study was conducted with soils sampled across five locations along a hydrological and topographical gradient ranging from a permafrost black spruce forest to a rich fen. The sites were situated within the Bonanza Creek Long-Term Ecological Research Station (LTER) site in interior Alaska (64.8° N and 148.0° W) (<http://www.lter.uaf.edu/data.cfm>). A boardwalk transect was constructed in 2005 that spanned the gradient from forest to fen. The transect included five distinct zones with varying plant communities and hydrology, which in the following are described in the same order as they appear along the gradient: A black spruce (*Picea Mariana*) forest with feathermoss and lichen ground cover; a bog birch site dominated by shrubs, including *Salix* spp. (willow) and *Betula* spp. (birch); a tussock grass site dominated by *Calamagrostis* spp. with a sparse covering of *Drepanocladus*; an emergent fen dominated by emergent species including *Equisetum* and *Carex* species, with a sparse cover of brown mosses; and a rich fen, which included a diverse ground layer mixture of *Sphagnum*, brown mosses and *Drepanocladus* spp., and a sparse cover of *Equisetum*. Transects perpendicular to the existing boardwalk were measured and soil cores were taken every 10 m

along transects. Five soil cores were taken at each transect down to 15 cm each representing a replicate ($n = 5$). Each soil core was taken with a 4 inch diameter sharpened steel core barrel attached to a cordless power drill. The soils were collected in July, 2008, and shipped to UC Berkeley, California, USA, where all analyses were conducted. Soil characteristics are given in Table 1.

Soil characteristics

Gravimetric water content was determined by drying soil to constant weight at 60°C. Loss on ignition was measured on dried soil after 6 h at 550°C.

Nucleic acid extraction

In short, soil community DNA was extracted from 0.2 g of soil with 1 ml of extraction buffer consisting of 400 µl 6.25 M ammonium acetate, 100 µl 1 M TRIS (pH 8), 40 µl 0.5 M EDTA (pH 8), and 460 µl double deionized water. To each tube 200 µl of silica beads (Biospec Products, Bartlesville, USA), 0.015 g of acid-washed PVPP, and 300 µl of chloroform: isoamylalcohol (24:1) (Lab Scan and Merck) were added followed by bead beating (30 s at 5.5 m s⁻¹) (BIO-101 bead beater, Savant, Holbrook, NY, USA). Supernatants were centrifuged for 20 min at 15 000 *g* to precipitate proteins. The new supernatants were transferred to 2 ml Eppendorf tubes, 100 µl 3 M sodium acetate (0.1× volume) was added, and the tubes were topped up with isopropyl alcohol (Sigma) (minimum 0.6× volume), vortexed and precipitated overnight (4°C). The samples were centrifuged (30 min, 15 000 *g*, 15°C) and the pellets were washed with ice-cold 75% ethanol and the DNA was dissolved in 100 µl double deionized water (Petersen *et al.*, 2004). The total amount of DNA was quantified spectrophotometrically using a NanoDrop ND-1000 spectrophotometer (NanoDrop Technologies) and diluted in MQ-water to a concentration of 2 ng µl⁻¹.

Quantitative PCR

Quantitative PCR (qPCR) was performed to assess the abundance of the following genes: the 16S rRNA gene (total bacterial and archaeal numbers), *amoA* gene (bacterial and archaeal ammonia oxidizers), *nirK* and *nirS* (nitrate reducers carrying a nitrite reductase gene) and *nosZ* (denitrifiers carrying the N₂O reductase gene). All qPCR reactions were conducted on an iCycler thermal cycler equipped with an optical module (Bio-Rad, USA). All samples were run in triplicate, and specific primer combinations and qPCR conditions are listed in Table 3. Single qPCR reactions were prepared in a total volume of 20 µl including 10 µl of iQ SYBR Green super mix (Bio-Rad), 4 µl of forward and reverse primers (3 µM) (Sigma-Aldrich), 1 µl PCR grade MQ-water (MP Bio-medicals) and 1 µl of template DNA (2 ng µl⁻¹). Presence of PCR inhibitors like co-extracted humic substances were tested by mixing known amounts of standard DNA in soil DNA extracts prior to qPCR, and comparing the quantification of standard DNA with and without DNA extracted from soil. We detected no inhibition of the qPCR assay with template DNA concentrations below 10 ng µl⁻¹. At the end of each qPCR

Table 3. Primers and thermal profiles used for real-time PCR quantification of the different phylogenetic and functional genes.

Target gene	Primers	Reference	Thermal profile	Number of cycles
16S rRNA gene	EUB338	Fierer <i>et al.</i> (2005)	95°C – 5 min	
	EUB518	Fierer <i>et al.</i> (2005)	95°C – 60 s/53°C – 30 s/72°C – 60 s	30
16S rRNA gene	Arch344	Mori <i>et al.</i> (2003)	95°C – 3 min	1
	Arch915	Mori <i>et al.</i> (2003)	95°C – 30 s/65°C – 30 s/72°C – 45 s	35
AOB <i>amoA</i>	amoA1F	Rotthauwe <i>et al.</i> (1997)	94°C – 5 min	1
	amoA2R	Rotthauwe <i>et al.</i> (1997)	94°C – 30 s/55°C – 45 s/72°C – 60 s	40
AOA <i>amoA</i>	Arch-amoAF	Francis <i>et al.</i> (2005)	94°C – 5 min	1
	Arch-amoAR	Francis <i>et al.</i> (2005)	94°C – 30 s/53°C – 45 s/72°C – 60 s	35
<i>nirK</i>	NirK876	Henry <i>et al.</i> (2004)	95°C – 5 min	1
	NirK1040	Henry <i>et al.</i> (2004)	95°C – 15 s/63 – 58°C – 30 s/72°C – 30 s	6 (touchdown)
			95°C – 15 s/58°C – 30 s/72°C – 30 s	40
<i>nirS</i>	Cd3aF	Michotey <i>et al.</i> (2000)	95°C – 5 min	1
	R3cd	Throback <i>et al.</i> (2004)	95°C – 15 s/63 – 58°C – 30 s/72°C – 30 s	6 (touchdown)
			95°C – 15 s/58°C – 30 s/72°C – 30 s	40
<i>nosZ</i>	NosZ2F	Henry <i>et al.</i> (2006)	95°C – 5 min	1
	NosZ2R	Henry <i>et al.</i> (2006)	95°C – 30 s/65 – 60°C – 30 s/72°C – 30 s	6 (touchdown)
			95°C – 15 s/60°C – 15 s/72°C – 30 s	40

run, a melting curve was conducted from 55 to 99°C with an increase of 0.5°C every 10 s, and purity of the amplified fragment was checked by the observation of a single melting peak. Also an agarose gel (1%) with the qPCR products were run to check for correct sized amplicon. PCR amplified DNA from environmental clones or cultured organisms was cleaned up with ExoSAP-IT (Affymetrix), and we generated standard curves based on quantified PCR product with a series of 1:10 dilutions. Standards were obtained from the following sources: *Bacillus* sp., culture (bacteria), environmental clones (archaea, bacterial *amoA*, archaeal *amoA* and *nirK*), and *Azoarcus* sp., culture (*nirS* and *nosZ*). Based on the dimensions of the core ($r = 5.08$ cm, depth = 15 cm) and the weight of each individual core (5 cores per site), DNA concentrations per gram of soil were transformed into DNA concentrations per area (ng m^{-2}). The abundances of relevant genes (copy numbers ng DNA^{-1}) were used calculate gene copy number m^{-2} down to 15 cm depth.

Soil contents of nitrate and ammonium and dissolved organic nitrogen (DON) and carbon (DOC)

Inorganic nitrogen (ammonium and nitrate) was determined colorimetrically for 5 replicates from each site. Five grams of fresh soil from the black spruce site, and 20 g from all the remaining sites was measured into 100 ml of 2 M KCl, the slurries were shaken for 1 h, then filtered through Whatman #1 papers. Ammonium and nitrate concentrations in the extracts were quantified by flow-injection analysis (Lachat QC8000, Hach Company, Loveland, CO, USA).

Dissolved organic nitrogen was measured colorimetrically on persulfate digests for 5 replicates from each site. Ten grams of fresh soil from the black spruce site, and 20 g from all the remaining sites was measured into 80 ml of 0.05 M K_2SO_4 . Slurries were shaken for 1 h, and then filtered through Whatman #1 filter papers. Two millilitres of the extract was digested with 8 ml deionized water and 10 ml of alkaline persulfate reagent (0.4 M NaOH + 0.2 M $\text{K}_2\text{S}_2\text{O}_8$ + 0.5 M H_3BO_4 , Fisher Scientific) in an autoclave at 0.1 MPa for 40 min (Yu *et al.*, 1994). The resulting NO_3^- in the digest was

quantified by flow-injection analysis (Hach Co, Loveland, CO, USA); inorganic N was subtracted from the total to yield DON. A separate aliquot of the extract was analysed for DOC using a model 1010 Total Inorganic Carbon/Total Organic Carbon analyser (OI Analytical, College Station, TX, USA).

Potential nitrification rates

Potential nitrification rates were determined for 5 replicates from each site, with 3 g moist soil from the black spruce site, and 8 g moist soil from all the remaining sites. One hundred millilitres of a solution of 1 mM phosphate buffer (0.3 mM KH_2PO_4 + 0.7 mM K_2HPO_4 , Fisher Scientific) at pH 7.2 and 0.5 mM $(\text{NH}_4)_2\text{SO}_4$ (Fisher Scientific) was added to each replicate followed by shaking at 150 r.p.m. at room temperature in aerobic flasks. At $T_{t=0}$, a 10 ml aliquot was transferred to a centrifuge tube, five drops of flocculent solution (0.5 M CaCl_2 + 0.5 M MgCl_2) (Fisher Scientific) was added to aliquots before centrifuging for 10 min at 3000 r.p.m. Five millilitres of clear supernatant were decanted and analysed for $\text{NO}_3^- + \text{NO}_2^-$ concentration by flow-injection analysis (Hach Co, Loveland, CO, USA). This procedure was repeated after 18 h of incubation ($T_{t=18}$) and PNR were calculated as differences in the concentration of $\text{NO}_3^- + \text{NO}_2^-$ between $T_{t=18}$ and $T_{t=0}$.

Potential denitrification rates (denitrification enzyme assay)

Potential denitrification rates were performed on five replicates from each site, with 5 g of moist soil from the black spruce site and 20 g of moist soil from the remaining sites in 225 ml jelly jars. Thirty millilitres of DEA solution (1 mM glucose and 1 mM KNO_3 , Fisher Scientific) was added to each replicate soil followed by a thorough shake. The headspace was flushed with N_2 three times and afterwards equilibrated with atmospheric pressure using a glass syringe. Twenty millilitres of headspace was removed and replaced by 20 ml of acetylene, after which initial samples were taken and

analysed immediately by pulsed-discharge detection (Valco Instruments, Houston, TX, USA) on a 6890 gas chromatograph (Agilent Technologies, Santa Clara, CA, USA). The soils were incubated for 45 min at 22°C on a rotary shaker (100 r.p.m.), after which final samples were taken and analysed. A control jar with 30 ml of DEA solution but no soil was included in the analysis.

Gross mineralization

Gross mineralization was measured using isotope dilution. Two millilitres of $(\text{NH}_4)_2\text{SO}_4$ (62.1 mg N l⁻¹ at 99 atom% ¹⁵N) was thoroughly mixed into 10 g of fresh soil from the black spruce site, and 30 g of fresh soil from the remaining sites. This difference in gram of soil was due to very low bulk density of the soil at the black spruce site, which was about 5 times lower compared with the rest of the sites. After 15 min to allow for abiotic reactions to occur, 8 g of soil from the black spruce site and 20 g of fresh soil from remaining sites was measured into 130 ml of 2 M KCl and shaken at 200 r.p.m. After 1 h, the soil slurries were filtered through Whatman #1 papers, and the extracts were stored frozen until further processing. The jars containing the remaining soil were covered with a polyethylene sheet and incubated for 9 h. At the end of incubation, soils were extracted and stored as above.

Ammonium concentrations in the extracts were analysed by flow-injection analysis (Hach, Loveland, CO, USA). Extracts were prepared for isotopic analysis by diffusion (Herman *et al.*, 1995). Samples were analysed on an automated nitrogen-carbon analyser coupled to an isotope ratio mass spectrometer (Sercon, Crewe, UK). Rates of gross ammonium production and consumption were estimated by standard isotopic dilution calculations (Hart *et al.*, 1994).

Statistics

Process rate measurements and microbial community information were calculated both per gram of soil as well as per m² of soil based upon soil bulk density numbers. There were no differences in the results or conclusions of the study between these two measurements and therefore we only present data per area (m²). Linear dependences between variables were described by correlations and Pearson's product-moment correlation coefficient (*r*) and *P*-values are given in Table 2. ANOVA tests followed by Tukey's honestly significance difference *post hoc* test (HSD) were used for each variable to analyse for significant differences among sites and *t*-tests were performed to analyse difference in gene abundances among sites.

We used a SMR model to analyse the best predictive variables for PNR and PDR, and tested a forward selection model as well as a combined forward selection and backward elimination model (mixed model), which yielded similar results. Path analysis was used to test possible causal relationships between physical/chemical and biological variables and potential rates of nitrification and denitrification. In path analysis, experimentally supported theory is used to formulate a conceptual model of the causal and non-causal relationships between the measured explanatory variables and their dependent variables. Experimental data are then used

to evaluate the models (e.g. Mitchell, 1992; Wootton, 1994). We devised two distinct full models with PNR or PDR as dependent variables, in which all relevant measured variables were included, and direct and indirect paths from each explanatory variable were appointed to evaluate the relationships between physical, chemical and biological explanatory variables on the potential process rate of interest in a theory constrained model. Reduced models were created by removing the paths with the largest probability values in a stepwise manner until all paths were significant (*P* < 0.05). Modification indices were used to determine if further addition or removal of paths would improve the reduced models. The full and reduced models were evaluated using multiple model-fit criteria. The model-fit criteria employed here can be separated into two general categories for evaluating theoretical models: model fit and model comparison. Chi-square (χ^2) and Tucker–Lewis NNFI were used to evaluate model fit, while LRT and Bentler CFI were used to compare alternative nested models. A non-significant *P*-value for model χ^2 indicates that the covariance pattern predicted by the model was not significantly different from the observed covariance, thus indicating a good fit of the model to the data (Shipley, 2000). Models with NNFI greater than 0.9 are considered acceptable since models with NNFI < 0.9 can usually be significantly improved (Bentler and Bonett, 1980). Likelihood ratio test is used to test for statistically significant differences in model fit, as determined by χ^2 , for two nested models and can be calculated as $\chi^2_{\text{initial}} - \chi^2_{\text{modified}}$ with degrees of freedom equal to d.f._{initial} - d.f._{modified}. A LRT that produces a statistically significant χ^2 at the 0.05 level of significance indicates that the two models are different (Schumacker and Lomax, 2010). The CFI values range from 0 to 1 and values greater than 0.95 are considered indicative of acceptable models (Shipley, 2000). It should be noted that path analysis is considered most appropriate for data sets with large sample sizes, which is not the case for our data set (*n* = 25). However, small sample sizes generally result in conservative fit estimates (Shipley, 2000).

In addition to evaluating model fit, path analysis quantifies the importance of each explanatory variable in explaining the variation in the dependent variables, which were PNR and PDR. The importance of the explanatory variables is based on the total effect of each explanatory variable and is the sum of direct and indirect pathways from the explanatory variables to the dependent variable. Direct effects represented by unidirectional arrows show the standardized partial regression coefficients (Wootton, 1994). The bidirectional arrows represent residual error and show the unexplained variance ($1 - R^2$) for each dependent variable. Path analyses were performed on variance–covariance matrices using the structural equation modelling function of the sem package in R (version 2.12.2) (Fox, 2006), and diagrams were generated using Graphviz. To account for disparate magnitudes of data, measurement scales were changed for appropriate data to bring all data to similar numeric magnitude prior to calculating variance–covariance matrices.

Acknowledgements

We would like to thank Marissa Lafler for her help with the DEA assays and inorganic nutrient analyses, Katie Shea

for helping out with the practical work on gross mineralization rates and Erin Nuccio for helping with qPCR assays. Also we thank Jennifer Harden and Dave McGuire (USGS) for designing and establishing the field sites. This project was funded by the Carlsberg foundation (reference: 2007_01_0395), the Bonanza Creek Long-Term Ecological Research program under National Science Foundation (Grant Nos. DEB-0620579, DEB-0423442, DEB-0080609, DEB-9810217, DEB-9211769, DEB-8702629), the Danish National Research Foundation and the Max Planck Society.

References

- Abell, G.C.J., Revill, A.T., Smith, C., Bissett, A.P., Volkman, J.K., and Robert, S.S. (2010) Archaeal ammonia oxidizers and *nirS*-type denitrifiers dominate sediment nitrifying and denitrifying populations in a subtropical macrotidal estuary. *ISME J* **4**: 286–300.
- Ambus, P., and Lowrance, R. (1991) Comparison of denitrification in 2 riparian soils. *Soil Sci Soc Am J* **55**: 994–997.
- Ambus, P., Mosier, A., and Christensen, S. (1992) Nitrogen turnover rates in a riparian fen determined by 15N dilution. *Biol Fertil Soils* **14**: 230–236.
- Attard, E., Recous, S., Chabbi, A., De Berranger, C., Guillaud, N., Labreuche, J., et al. (2011) Soil environmental conditions rather than denitrifier abundance and diversity drive potential denitrification after changes in land uses. *Global Change Biol* **17**: 1975–1989.
- Babic, K.H., Schauss, K., Hai, B., Sikora, S., Redzepovic, S., Radl, V., and Schloter, M. (2008) Influence of different *Sinorhizobium meliloti* inocula on abundance of genes involved in nitrogen transformations in the rhizosphere of alfalfa (*Medicago sativa* L.). *Environ Microbiol* **10**: 2922–2930.
- Baudoin, E., Philippot, L., Cheneby, D., Chapuis-Lardy, L., Fromin, N., Bru, D., et al. (2009) Direct seeding mulch-based cropping increases both the activity and the abundance of denitrifier communities in a tropical soil. *Soil Biol Biochem* **41**: 1703–1709.
- Bayley, S.E., Thormann, M.N., and Szumigalski, A.R. (2005) Nitrogen mineralization and decomposition in western boreal bog and fen peat. *Ecoscience* **12**: 455–465.
- Bengtsson, G., Bengtson, P., and Mansson, K.F. (2003) Gross nitrogen mineralization-, immobilization-, and nitrification rates as a function of soil C/N ratio and microbial activity. *Soil Biol Biochem* **35**: 143–154.
- Bentler, P.M., and Bonett, D.G. (1980) Significance tests and goodness of fit in the analysis of covariance structures. *Psychol Bull* **88**: 588–606.
- Bernhard, A.E., Landry, Z.C., Blevins, A., Torre, J.R., Giblin, A.E., and Stahl, D.A. (2010) Abundance of ammonia-oxidizing archaea and bacteria along an estuarine salinity gradient in relation to potential nitrification rates. *Appl Environ Microbiol* **76**: 1285–1289.
- Biasi, C., Meyer, H., Rusalimova, O., Hammerle, R., Kaiser, C., Baranyi, C., et al. (2008) Initial effects of experimental warming on carbon exchange rates, plant growth and microbial dynamics of a lichen-rich dwarf shrub tundra in Siberia. *Plant Soil* **307**: 191–205.
- Boyle-Yarwood, S.A., Bottomley, P.J., and Myrold, D.D. (2008) Community composition of ammonia-oxidizing bacteria and archaea in soils under stands of red alder and Douglas fir in Oregon. *Environ Microbiol* **10**: 2956–2965.
- Bremer, C., Braker, G., Matthies, D., Beierkuhnlein, C., and Conrad, R. (2009) Plant presence and species combination, but not diversity, influence denitrifier activity and the composition of *nirK*-type denitrifier communities in grassland soil. *FEMS Microbiol Ecol* **70**: 377–387.
- Carney, K.M., Matson, P.A., and Bohannan, B.J.M. (2004) Diversity and composition of tropical soil nitrifiers across a plant diversity gradient and among land-use types. *Ecol Lett* **7**: 684–694.
- Chapin, D.M. (1996) Nitrogen mineralization, nitrification, and denitrification in a high arctic lowland ecosystem, Devon Island, NWT, Canada. *Arctic Alpine Res* **28**: 85–92.
- Chronakova, A., Radl, V., Cuhel, J., Simek, M., Elhottova, D., Engel, M., and Schloter, M. (2009) Overwintering management on upland pasture causes shifts in an abundance of denitrifying microbial communities, their activity and N₂O-reducing ability. *Soil Biol Biochem* **41**: 1132–1138.
- Cuhel, J., Simek, M., Laughlin, R.J., Bru, D., Cheneby, D., Watson, C.J., and Philippot, L. (2010) Insights into the effect of soil pH on N₂O and N₂ emissions and denitrifier community size and activity. *Appl Environ Microbiol* **76**: 1870–1878.
- Dandie, C.E., Burton, D.L., Zebarth, B.J., Henderson, S.L., Trevors, J.T., and Goyer, C. (2008) Changes in bacterial denitrifier community abundance over time in an agricultural field and their relationship with denitrification activity. *Appl Environ Microbiol* **74**: 5997–6005.
- Desnues, C., Michotey, V.D., Wieland, A., Zhizang, C., Fourcans, A., Duran, R., and Bonin, P.C. (2007) Seasonal and diel distributions of denitrifying and bacterial communities in a hypersaline microbial mat (Camargue, France). *Water Res* **41**: 3407–3419.
- Di, H.J., Cameron, K.C., Shen, J.P., Winefield, C.S., O'Callaghan, M., Bowatte, S., and He, J.Z. (2009) Nitrification driven by bacteria and not archaea in nitrogen-rich grassland soils. *Nat Geosci* **2**: 621–624.
- Dijgal, D., Baudoin, E., Philippot, L., Brauman, A., and Villenave, C. (2010) Shifts in size, genetic structure and activity of the soil denitrifier community by nematode grazing. *Eur J Soil Biol* **46**: 112–118.
- Dong, L.F., Smith, C.J., Papaspyrou, S., Stott, A., Osborn, A.M., and Nedwell, D.B. (2009) Changes in benthic denitrification, nitrate ammonification, and anammox process rates and nitrate and nitrite reductase gene abundances along an estuarine nutrient gradient (the Colne Estuary, United Kingdom). *Appl Environ Microbiol* **75**: 3171–3179.
- Fierer, N., Schimel, J.P., Cates, R.G., and Zou, J.P. (2001) Influence of balsam poplar tannin fractions on carbon and nitrogen dynamics in Alaskan taiga floodplain soils. *Soil Biol Biochem* **33**: 1827–1839.
- Fierer, N., Jackson, J.A., Vilgalys, R., and Jackson, R.B. (2005) Assessment of soil microbial community structure by use of taxon-specific quantitative PCR assays. *Appl Environ Microbiol* **71**: 4117–4120.
- Fox, J. (2006) Structural equation modeling with the sem package in R. *Struct Equation Model* **13**: 465–486.
- Francis, C.A., Roberts, K.J., Beman, J.M., Santoro, A.E., and Oakley, B.B. (2005) Ubiquity and diversity of ammonia-

- oxidizing archaea in water columns and sediments of the ocean. *Proc Natl Acad Sci USA* **102**: 14683–14688.
- Giblin, A.E., Nadelhoffer, K.J., Shaver, G.R., Laundre, J.A., and Mckerrow, A.J. (1991) Biogeochemical diversity along a riverside toposequence in Arctic Alaska. *Ecol Monogr* **61**: 415–435.
- Groffman, P.M., and Crawford, M.K. (2003) Denitrification potential in urban riparian zones. *J Environ Qual* **32**: 1144–1149.
- Groffman, P.M., Altabet, M.A., Bohlke, J.K., Butterbach-Bahl, K., David, M.B., Firestone, M., *et al.* (2006) Methods for measuring denitrification: diverse approaches to a difficult problem. *Ecol Appl* **16**: 2091–2122.
- Hallin, S., Jones, C.M., Schloter, M., and Philippot, L. (2009) Relationship between N-cycling communities and ecosystem functioning in a 50-year-old fertilization experiment. *ISME J* **3**: 597–605.
- Hart, S.C., Stark, J.M., Davidson, E.A., and Firestone, M.K. (1994) Nitrogen mineralization, immobilization, and nitrification. In *Methods of Soil Analysis Part 2*. Weaver, R.W., Angle, S., Bottomley, P., Bezdiecek, D., Smith, S., Tabatabai, A., and Wollum, A. (eds). Madison, WI, USA: SSSA, pp. 985–1018.
- He, J., Shen, J., Zhang, L., Zhu, Y., Zheng, Y., Xu, M., and Di, H.J. (2007) Quantitative analyses of the abundance and composition of ammonia-oxidizing bacteria and ammonia-oxidizing archaea of a Chinese upland red soil under long-term fertilization practices. *Environ Microbiol* **9**: 2364–2374.
- Henry, S., Baudoin, E., Lopez-Gutierrez, J.C., Martin-Laurent, F., Baumann, A., and Philippot, L. (2004) Quantification of denitrifying bacteria in soils by *nirK* gene targeted real-time PCR. *J Microbiol Methods* **59**: 327–335.
- Henry, S., Bru, D., Stres, B., Hallet, S., and Philippot, L. (2006) Quantitative detection of the *nosZ* gene, encoding nitrous oxide reductase, and comparison of the abundances of 16S rRNA, *narG*, *nirK*, and *nosZ* genes in soils. *Appl Environ Microbiol* **72**: 5181–5189.
- Herman, D.J., Brooks, P.D., Ashraf, M., Azam, F., and Mulvaney, R.L. (1995) Evaluation of methods for N-15 analysis of inorganic nitrogen in soil extracts. 2. Diffusion methods. *Commun Soil Sci Plant Anal* **26**: 1675–1685.
- Hoffmann, H., Schloter, M., and Wilke, B.M. (2007) Microscale-scale measurement of potential nitrification rates of soil aggregates. *Biol Fertil Soils* **44**: 411–413.
- Jia, Z.J., and Conrad, R. (2009) Bacteria rather than Archaea dominate microbial ammonia oxidation in an agricultural soil. *Environ Microbiol* **11**: 1658–1671.
- Junier, P., Kim, O.S., Witzel, K.P., Imhoff, J.F., and Hadas, O. (2008) Habitat partitioning of denitrifying bacterial communities carrying *nirS* or *nirK* genes in the stratified water column of Lake Kinneret, Israel. *Aquat Microb Ecol* **51**: 129–140.
- Kaiser, C., Meyer, H., Biasi, C., Rusalimova, O., Barsukov, P., and Richter, A. (2005) Storage and mineralization of carbon and nitrogen in soils of a frost-boil tundra ecosystem in Siberia. *Appl Soil Ecol* **29**: 173–183.
- Kim, S.Y., Lee, S.H., Freeman, C., Fenner, N., and Kang, H. (2008) Comparative analysis of soil microbial communities and their responses to the short-term drought in bog, fen, and riparian wetlands. *Soil Biol Biochem* **40**: 2874–2880.
- Klingensmith, K.M., and Van Cleve, K. (1993) Patterns of nitrogen mineralization and nitrification in floodplain successional soils along the Tanana river, interior Alaska. *Can J For Res* **23**: 964–969.
- Knapp, C.W., Dodds, W.K., Wilson, K.C., O'Brien, J.M., and Graham, D.W. (2009) Spatial heterogeneity of denitrification genes in a highly homogenous urban stream. *Environ Sci Technol* **43**: 4273–4279.
- Le Roux, X., Poly, F., Currey, P., Commeaux, C., Hai, B., Nicol, G., *et al.* (2008) Effects of aboveground grazing on coupling among nitrifier activity, abundance and community structure. *ISME J* **2**: 221–232.
- Leininger, S., Urich, T., Schloter, M., Schwark, L., Qi, J., Nicol, G., *et al.* (2006) Archaea predominate among ammonia-oxidizing prokaryotes in soils. *Nature* **442**: 806–809.
- Makarov, M.I., Glaser, B., Zech, W., Malysheva, T.I., Bulatnikova, I.V., and Volkov, A.V. (2003) Nitrogen dynamics in alpine ecosystems of the northern Caucasus. *Plant Soil* **256**: 389–402.
- Mertens, J., Broos, K., Wakelin, S.A., Kowalchuk, G.A., Springael, D., and Smolders, E. (2009) Bacteria, not archaea, restore nitrification in a zinc-contaminated soil. *ISME J* **3**: 916–923.
- Michotey, V., Mejean, V., and Bonin, P. (2000) Comparison of methods for quantification of cytochrome cd₁-denitrifying bacteria in marine samples. *Appl Environ Microbiol* **66**: 1564–1571.
- Miller, M.N., Zebarth, B.J., Dandie, C.E., Burton, D.L., Goyer, C., and Trevors, J.T. (2008) Crop residue influence on denitrification, N₂O emissions and denitrifier community abundance in soil. *Soil Biol Biochem* **40**: 2553–2562.
- Mitchell, R.J. (1992) Testing evolutionary and ecological hypotheses using path-analysis and structural equation modeling. *Funct Ecol* **6**: 123–129.
- Mori, K., Kim, H., Kakegawa, T., and Hanada, S. (2003) A novel lineage of sulfate-reducing microorganisms: thermodesulfobiaceae fam. nov., *Thermodesulfobium narugense*, gen. nov., sp nov., a new thermophilic isolate from a hot spring. *Extremophiles* **7**: 283–290.
- Mosier, A.R. (1998) Soil processes and global change. *Biol Fertil Soils* **27**: 221–229.
- Nogales, B., Timmis, K.N., Nedwell, D.B., and Osborn, A.M. (2002) Detection and diversity of expressed denitrification genes in estuarine sediments after reverse transcription-PCR amplification from mRNA. *Appl Environ Microbiol* **68**: 5017–5025.
- Petersen, D.G., Dahllöf, I., and Nielsen, L.P. (2004) Effects of zinc pyriithione and copper pyriithione on microbial community function and structure in sediments. *Environ Toxicol Chem* **23**: 921–928.
- Philippot, L., Cuhel, J., Saby, N.P.A., Cheneby, D., Chronakova, A., Bru, D., *et al.* (2009) Mapping field-scale spatial patterns of size and activity of the denitrifier community. *Environ Microbiol* **11**: 1518–1526.
- Prather, M., Ehhalt, D., Dentener, F., Derwent, R., Dlugokencky, E., Holland, E., *et al.* (2001) Atmospheric chemistry and greenhouse gases. In *Climate Change 2001: The Scientific Basis Contribution of Working Group I to the Third Assessment Report of the Intergovernmental Panel on Climate Change*. Houghton, J.T., Ding, Y., Griggs, D.,

- Noguer, M., van der Linden, P., Dai, X., *et al.* (eds). Cambridge, UK: Cambridge University Press, pp. 239–280.
- Ravishankara, A.R., Daniel, J.S., and Portmann, R.W. (2009) Nitrous oxide (N₂O): the dominant ozone-depleting substance emitted in the 21st century. *Science* **326**: 123–125.
- Rotthauwe, J.H., Witzel, K.P., and Liesack, W. (1997) The ammonia monooxygenase structural gene *amoA* as a functional marker: molecular fine-scale analysis of natural ammonia-oxidizing populations. *Appl Environ Microbiol* **63**: 4704–4712.
- Schipper, L.A., Cooper, A.B., Harfoot, C.G., and Dyck, W.J. (1993) Regulators of denitrification in an organic riparian soil. *Soil Biol Biochem* **25**: 925–933.
- Schumacker, R.E., and Lomax, R.G. (2010) *A Beginner's Guide to Structural Equation Modelling*. New York, USA: Taylor and Francis Group.
- Shen, J., Zhang, L., Zhu, Y., Zhang, J., and He, J. (2008) Abundance and composition of ammonia-oxidizing bacteria and ammonia-oxidizing archaea communities of an alkaline sandy loam. *Environ Microbiol* **10**: 1601–1611.
- Shipley, B. (2000) *Cause and Correlation in Biology: A User's Guide to Path Analysis, Structural Equations, and Causal Inference*. Cambridge, UK: Cambridge University Press.
- Smith, J.M., and Ogram, A. (2008) Genetic and functional variation in denitrifier populations along a short-term restoration chronosequence. *Appl Environ Microbiol* **74**: 5615–5620.
- Song, K., Lee, S.H., Mitsch, W.J., and Kang, H. (2010) Different responses of denitrification rates and denitrifying bacterial communities to hydrologic pulsing in created wetlands. *Soil Biol Biochem* **42**: 1721–1727.
- Throback, I.N., Enwall, K., Jarvis, A., and Hallin, S. (2004) Reassessing PCR primers targeting *nirS*, *nirK* and *nosZ* genes for community surveys of denitrifying bacteria with DGGE. *FEMS Microbiol Ecol* **49**: 401–417.
- Van Cleve, K., Yarie, J., Erickson, R., and Dyrssen, D. (1993) Nitrogen mineralization and nitrification in successional ecosystems of the Tanana River floodplain, interior Alaska. *Can J Forest Res* **23**: 970–978.
- Wallenstein, M.D., Myrold, D.D., Firestone, M., and Voytek, M. (2006) Environmental controls on denitrifying communities and denitrification rates: insights from molecular methods. *Ecol Appl* **16**: 2143–2152.
- Wankel, S.D., Mosier, A.C., Hansel, C.M., Paytan, A., and Francis, C.A. (2011) Spatial variability in nitrification rates and ammonia-oxidizing microbial communities in the agriculturally impacted Elkhorn Slough Estuary, California. *Appl Environ Microbiol* **77**: 269–280.
- Wheatley, R.E., and Williams, B.L. (1989) Seasonal changes in rates of potential denitrification in poorly-drained reseeded blanket peat. *Soil Biol Biochem* **21**: 355–360.
- Wootton, J.T. (1994) Predicting direct and indirect effects – an integrated approach using experiments and path-analysis. *Ecology* **75**: 151–165.
- Wray, H.E., and Bayley, S.E. (2007) Denitrification rates in marsh fringes and fens in two boreal peatlands in Alberta, Canada. *Wetlands* **27**: 1036–1045.
- Yu, Z.S., Northup, R.R., and Dahlgren, R.A. (1994) Determination of dissolved organic nitrogen using persulfate oxidation and conductimetric quantification of nitrate-nitrogen. *Commun Soil Sci Plant Anal* **25**: 3161–3169.
- Zumft, W.G. (1997) Cell biology and molecular basis of denitrification. *Microbiol Mol Biol Rev* **61**: 533–616.